Microwave Spectrum of [1,1]-Pyridine−Ne_2[†]

Luca Evangelisti,[‡] Laura B. Favero,[§] Barbara M. Giuliano,[‡] Shouyuan Tang,[‡,||] Sonia Melandri,[‡] and Walther Caminati*[,‡]

Dipartimento di Chimica "G. Ciamician" dell'Università di Bologna, Via Selmi 2, I-40126 Bologna, Italy, and Istituto per lo Studio dei Materiali Nanostrutturati (Sezione di Bologna), Consiglio Nazionale delle Ricerche, Via Gobetti 101, I-40129 Bologna, Italy

Received: March 5, 2009; Revised Manuscript Received: April 20, 2009

We investigated the rotational spectra of six isotopologues of pyridine−Ne_2, formed by combinations of two isotopes of the nitrogen atom (^{14}N and ^{15}N) in pyridine with two isotopes of the rare gas atoms (^{20}Ne and ^{22}Ne), by using pulsed jet Fourier transform microwave spectroscopy. We detected the C_{2v} symmetry conformer, denoted as [1,1], where the Ne atoms are located one on each side of the ring plane. The [2,0] species, with the two Ne atoms on the same side of the ring, was not observed. Two structural parameters, R and θ, that localize the rare gas atoms with respect to pyridine have been determined. The ^{14}N nuclear quadrupole coupling constants have been obtained for the isotopologues containing this nucleus.

Introduction

Several complexes between aromatic molecules and rare gas (RG) atoms have been studied by microwave spectroscopy.[1] The complexes with benzene (Bz) can be considered as prototype systems for this family of adducts. The rotational spectra of Bz−Ne,[2,3] Bz−Ar,[3,4] Bz−Kr,[5] and Bz−Xe[3] have been observed by Fourier transform microwave (FTMW) spectroscopy. Only the rotational spectrum of the adduct Bz−He has not yet been reported, due to its very low stability. In the case of pyridine (Py), microwave spectra have been reported for the 1:1 complexes with all rare gases.[6−11]

The high resolution of the FTMW technique gives us the opportunity to study the effect of weak intermolecular interactions in van der Waals clusters. Information on the potential energy surfaces of the van der Waals motions have been obtained according to the pseudo-diatomic approximation[12] and/or by use of some other models, such as fitting of the potential energy surface (PES) directly to the observed rotational transition frequencies (an analytic representation of this PES and a dynamical model of the complex are needed in this case[13]), or from Coriolis and mass dispersion effects related to the rare gas atom vibrations parallel to the ring plane.[14]

A molecular complex constituted of two RG atoms attached to an aromatic frame becomes more complicated either from a structural/conformational or from a dynamics point of view. Two conformers, denoted as [1,1] or [2,0], depending on the fact that the two RG atoms are located on two different sides (above and below) or on the same side of the aromatic ring plane, can exist. So far, pure rotational spectra have been observed only for pyridine−Ar_2[10] and furan−Ar_2.[15] In both cases only the [1,1] form has been detected. Also the rotationally resolved spectra of two vibronic bands of Bz−Ar_2 revealed only the [1,1] conformer.[16]

A theoretical study, based on atom-bond additive potentials for Bz−RG clusters and on dynamics simulations, indicates that the [1,1] form is much more abundant when $T < 10-50$ K (the wide range depending on the RG atom),[17] so that, at the temperatures reached in a supersonic expansion, only this conformer should be observed.

However, rotational contour studies of the UV vibronic bands of the Bz−Ar_2 complex in supersonic expansions give experimental evidence of both [1,1] and [2,0] conformers.[18,19] This is probably due to the fact that during the adiabatic expansion the conformational relaxation process is not sufficiently fast.

Since the Ne atom is smaller than Ar, the possibility to allocate two atoms on the same side of an aromatic plane might be higher and thus we decided to investigate the rotational spectrum of Py−Ne_2. Such a study should then provide experimental data to better understand many-body nonadditive contributions in intermolecular interactions.

We report here the microwave spectra of six isotopologues of Py−Ne_2 deriving from the combinations of two isotopes of both gases, the nitrogen atom (^{14}N and ^{15}N) in pyridine and ^{20}Ne and ^{22}Ne in the rare gas. The geometrical structure of the complex and its ^{14}N nuclear quadrupole coupling constants are discussed. The principal axis system of Py−Ne_2 is shown in Figure 1.

Experimental Section

The rotational spectra were measured in the 6.0−18.0 GHz frequency range with a COBRA-type[20] pulsed supersonic-jet Fourier transform microwave (FTMW) spectrometer[21] described elsewhere.[22] van der Waals complexes were formed by expanding a gas mixture of 0.5% pyridine in neon at room temperature and at a backing pressure of about 2×10^5 Pa, through the pulsed valve (General valve, series 9, nozzle diameter 0.5 mm) into the Fabry−Perot cavity to about 1×10^{-3} Pa. The spectral line position was determined after Fourier transformation of the 8K data point time domain signal, recorded at intervals of 100 ns. Each rotational transition is split by Doppler effect as a result of the coaxial arrangement of the supersonic jet and resonator axes in the COBRA-FTMW spectrometer. The rest frequency is calculated as the arithmetic mean of the Doppler components.

[†] Part of the Vincenzo Aquilanti Festschrift.

* Corresponding author: phone +39-051-2099480; fax +39-051-2099456; e-mail walther.caminati@unibo.it.

[‡] Dipartimento di Chimica "G. Ciamician" dell'Università di Bologna.

[§] ISMN (Sezione di Bologna), CNR.

[||] Permanent address: College of Bioengineering, ChongQing University, ChongQing 400044, P. R. China.

10.1021/jp902034k
Published on Web 05/28/2009

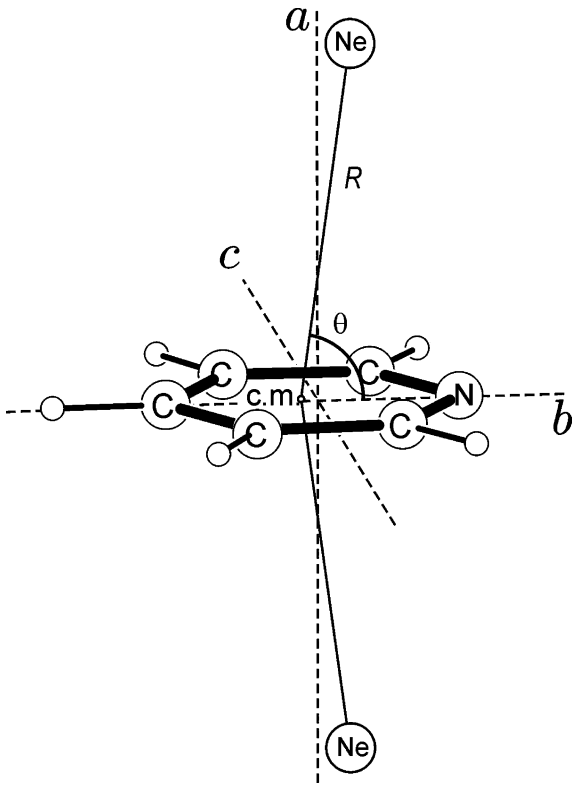

Figure 1. Structural parameters and coordinate system for the pyridine−Ne_2 complex. c.m. represents the center of mass in isolated pyridine.

The estimated accuracy of frequency measurements is better than 3 kHz, and lines separated by more than 7 kHz are resolvable. (^{15}N)Pyridine (98%) was obtained from Aldrich and used without further purification.

Results and Discussion

Rotational Spectra and Analysis. The rotational constants of Py−Ne_2 were estimated from the geometry reported for the Py−Ne complex,[8] imposing a C_{2v} symmetry. A second neon atom was bound to an equivalent position on the opposite side of the ring plane. This geometry is similar to those of Py−Ar_2[10] and furan−Ar_2.[15] The orientation of the principal axis system of pyridine changes in the complex. The order of the principal axes is permuted from *abc* in the monomer to *bca* in the complex. As a consequence, the dipole moment of Py−Ne_2 lies only along the *b* axis.

The hyperfine structure due to the presence of the ^{14}N nucleus has been interpreted on the basis of the previously determined quadrupole coupling tensor for the complex (^{14}N)Py−^{20}Ne.[8]

Some 55, 49, and 7 μ_b-type transitions were measured for the (^{14}N)Py−^{20}Ne^{20}Ne, (^{14}N)Py−^{20}Ne^{22}Ne, and (^{14}N)Py−^{22}Ne^{22}Ne isotopologues, respectively.

A statistical weight of 10:6, depending on the parity of the sum ($K_a + K_c$), was observed in the symmetric species (^{20}Ne^{20}Ne or ^{22}Ne^{22}Ne), as will be discussed in a subsequent paragraph.

Figure 2 (top) shows the unusual intensities of the transitions of the ^{22}Ne-containing isotopologues, which are discussed below.

All experimental frequencies were fitted by use of Pickett's SPFIT program[23] according to the Hamiltonian:

$$H = H_R + H_{CD} + H_Q \quad (1)$$

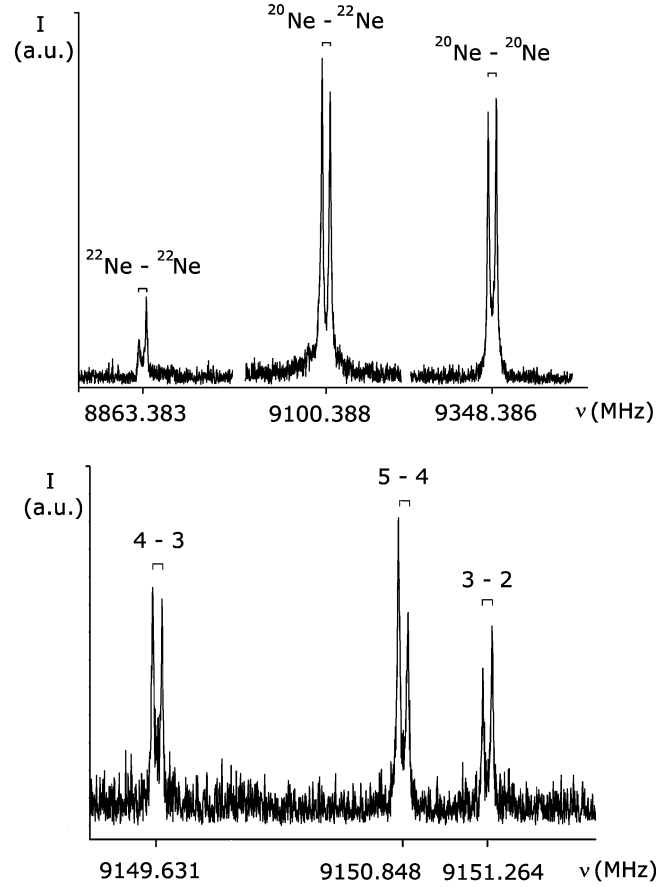

Figure 2. Recorded $4_{14}-3_{03}$ transitions of four isotopologues (the transition notation is $J'_{K_a'K_c'} \leftarrow J''_{K_a''K_c''}$). The unusual high intensities of the ^{22}Ne species are outlined at the top for the complexes with (^{15}N)Py. At the bottom, the triplet feature (F′←F″) due to the ^{14}N quadrupolar interaction is shown for the (^{14}N)Py−^{20}Ne^{20}Ne species.

where H_R, H_{CD}, and H_Q are the rotational, centrifugal distortion, and nuclear quadrupole coupling contributions to the total Hamiltonian. Matrix elements of H_Q were valuated in the coupled basis set $F = J + I_{N(14)}$. Since Py−Ne_2 is a nearly prolate molecule, Watson's *S*-reduction and I^r representation[24] were chosen. Using a sample of pyridine enriched in ^{15}N, we assigned the spectra of (^{15}N)Py−^{20}Ne^{20}Ne, (^{15}N)Py−^{20}Ne^{22}Ne, and (^{15}N)Py−^{22}Ne^{22}Ne. These spectra are simpler because ^{15}N has only a magnetic moment, together with a quantum number $I = {}^1/_2$ for the nuclear spin, so that the hyperfine structure disappears. We measured 24, 22, and 11 μ_b-type transitions for the three isotopologues, which were fitted with a simplified Hamiltonian, with H_Q omitted in eq 1. All experimental frequencies are available as Supporting Information, and the spectroscopic constants with their uncertainties are summarized in Table 1.

Statistical Weight. An intensity ratio 10/6 in favor of the transitions with even values for ($K_a + K_c$) is observed. The complex Py−Ne_2 possesses a C_{2v} symmetry axis that lies along the *b* principal axis. The corresponding $\hat{C}_2$ symmetry operation interchanges—for the most abundant species—three pairs of equivalent bosons (^{20}Ne^{20}Ne, ^{12}C2^{12}C6, and ^{12}C3^{12}C5) and two pairs of equivalent fermions (H2H6 and H3H5), so that the Bose−Einstein statistics hold. Then, the overall wave function,

$$\psi_{tot} = \psi_e\psi_v\psi_R\psi_s \quad (2)$$

must be symmetric. Both electronic (ψ_e) and vibrational (ψ_v) wave functions are symmetric for the ground state. The spin

TABLE 1: Spectroscopic Constants of All Measured Isotopologues of Py−Ne_2

	(^{14}N)Py−^{20}Ne^{20}Ne	(^{14}N)Py−^{20}Ne^{22}Ne	(^{14}N)Py−^{22}Ne^{22}Ne	(^{15}N)Py−^{20}Ne^{20}Ne	(^{15}N)Py−^{20}Ne^{22}Ne	(^{15}N)Py−^{22}Ne^{22}Ne
A/MHz	2957.3943(2)[a]	2956.4767(5)	2955.476(1)	2928.2562(6)	2927.4510(5)	2926.5808(4)
B/MHz	931.5448(2)	895.2182(4)	860.595(4)	931.7995(3)	895.4580(3)	860.7832(5)
C/MHz	922.5443(1)	886.8243(3)	852.755(1)	919.8770(3)	884.3747(2)	850.4672(3)
D_J/kHz	3.617(2)	3.320(6)	[3.617][b]	3.594(4)	3.350(3)	3.14(7)
D_{JK}/kHz	18.09(2)	17.17(2)	[18.09]	18.07(2)	16.76(2)	15.57(2)
D_K/kHz	−14.06(2)	−12.70(4)	[−14.06]	−15.12(6)	−13.28(4)	−11.62(4)
d_1/kHz	0.027(5)	[0.027]	[0.027]	0.039(4)	0.033(2)	0.042(3)
χ_{aa}/MHz	3.411(2)	3.411(4)	[3.411]			
χ^{-}[c]/MHz	−6.296(2)	−6.296(8)	[−6.296]			
σ/kHz[d]	1	6	3	2	2	1
N[e]	55	49	7	24	22	11

[a] Errors in parentheses are expressed in unit of the last digit. [b] Values shown in square brackets are undetermined in the fit and fixed at the value of the normal species. [c] $\chi^{-} = (\chi_{bb} - \chi_{cc})$. [d] Standard deviation of the fit. [e] Number of transitions in the fit.

TABLE 2: Intensities,[a] Transitions, and Natural Abundances of Py(^{15}N)Py−^{20}Ne^{20}Ne, (^{15}N)Py−^{20}Ne^{22}Ne, and (^{15}N)Py−^{22}Ne^{22}Ne Species

	Py−^{20}Ne^{20}Ne	Py−^{20}Ne^{22}Ne	Py−^{22}Ne^{22}Ne
natural statistical abundance	0.81	0.18	0.01
experimental relative intensities	1.00	0.37(5)	0.26(9)

[a] Averaged over seven transitions.

TABLE 3: Planar Moments of Observed Pyridine Monomers and Pyridine Complex

	x	*y*	*z*	P_{xx}/uÅ^2	P_{yy}/uÅ^2	P_{zz}/uÅ^2	ref
(^{14}N)Py	*a*	*b*	*c*	87.0800	83.7018	−0.0193	26
(^{14}N)Py−^{20}Ne	*b*	*c*	*a*	85.2385	82.5800	186.7537	8
(^{14}N)Py−^{20}Ne$_2$	*b*	*c*	*a*	88.0897	82.7969	459.7203	this work

TABLE 4: r_s Coordinates of the Ne and N Atoms from Some Combinations of Isotopic Species ([a])

atom	parent	substituted species	|*a*|	|*b*|
N	(^{14}N)Py−^{20}Ne^{20}Ne	(^{15}N)Py−^{20}Ne^{20}Ne	0.38i(1)	1.311(1)
N	(^{14}N)Py−^{22}Ne^{22}Ne	(^{15}N)Py−^{22}Ne^{22}Ne	0.36i(1)	1.306(1)
Ne	(^{14}N)Py−^{20}Ne^{20}Ne	(^{14}N)Py−^{22}Ne^{20}Ne	3.346(1)	0.17(2)
Ne	(^{14}N)Py−^{20}Ne^{20}Ne	(^{14}N)Py−^{22}Ne^{22}Ne[b]	3.345(1)	0.17(2)

[a] Coordinate *c* is fixed to zero by symmetry. [b] Requires double substitution procedure.[28]

function ψ_s (10 A_1; 6 B_1) has a ratio 5/3 between symmetric and antisymmetric components. With the C_2 symmetry axis lying along the *b*-axis, the even rotational functions are characterized by an even value of $(K_a + K_c)$, and vice versa. Thus, the rotational transitions with a symmetric initial state ψ_R will have a favorable intensity ratio of 5/3 with respect to the antisymmetric ones. The observed intensity variations are consistent with the above considerations.

Unusual High Intensities of Transitions of the ^{22}Ne Species. As shown in the upper part of Figure 2, where the intensities of the $4_{14}-3_{03}$ transitions of the ^{20}Ne^{20}Ne, ^{20}Ne^{22}Ne, and ^{22}Ne^{22}Ne isotopologues with (^{15}N)Py are represented, it turns out that there is significant enrichment of the heavier isotopomers in the molecular expansion. We measured relative intensities of the three isotopologues for seven transitions, three of them with even and four with odd starting rotational states, and after corrections for the statistical weights, we found the relative intensities reported in Table 2, together with the natural abundances of the three species.

It turns out that in the jet conditions the ground-state populations of the Py−^{20}Ne^{22}Ne and Py−^{22}Ne^{22}Ne isotopologues increase by factors of ≈2 and ≈20, respectively, with respect to that of the normal (Py−^{20}Ne^{20}Ne) species. The mass increase for the heavier isotopomers results in a lower zero-point energy level and larger dissociation energy. Then, the isotopic enrichment can be explained by the thermal quasi-equilibrium reached as a result of repeated dissociation and re-formation of the trimers in the low-temperature molecular expansion.[25]

Structure. It is common to describe the equilibrium structure of the complex between an aromatic molecule and a rare gas atom with the structural parameters *R* and θ (see Figure 1). *R* measures the distance between the center of mass of the aromatic monomer and the rare gas atom, while θ is the angle between *R* and the principal axis *a* of isolated pyridine. These parameters can be used for [1,1] complexes between pyridine and two gas atoms of neon located symmetrically on both sides of the aromatic ring plane. As described before, the principal axis system changes between monomer and complex. It is well-known that both Coriolis and mass dispersion effects related to the rare gas atom bendings contribute to the effective moments of inertia. If we take into account the planar moments of inertia:

$$P_{aa} = \sum_i m_i a_i^2 = \frac{h}{16\pi^2}\left(-\frac{1}{A} + \frac{1}{B} + \frac{1}{C}\right) \qquad \text{etc.} \qquad (3)$$

and use the subscripts *xx*, *yy*, and *zz* (rather than *aa*, *bb*, and *cc*) in order to take into account the changes in the principal axes systems in going from Py to Py−Ne and Py−Ne_2 (see Table 3), we can see that the P_{zz} values increase from ca. 0 to the values corresponding to the increase of the mass extensions out of the plane, while the P_{yy} has unexpected reductions, especially for the 1:1 adduct (in this last case also P_{xx} decreases). Such a kind of diminution has been used to obtain information—with a 2D flexible model—on the potential energy surface of the van der Waals bendings. In the case of the trimer, these diminutions are less marked, and in any case four-dimensional models would be required to interpret the Coriolis and mass dispersion effects related to the bending motions of two rare gas atoms.

We can combine the rotational constants of the various isotopic species in various ways, in order to obtain quantitative structural information by Kraitchman's equations.[27] There are several possible combinations of parent/substituted species. We report in Table 4 the r_s coordinates of the N atom derived from the pairs (^{14}N)Py−^{20}Ne^{20}Ne/(^{15}N)Py−^{20}Ne^{20}Ne, and (^{14}N)Py−^{22}Ne^{22}Ne/(^{15}N)Py−^{22}Ne^{22}Ne, and the r_s coordinates of the Ne atom derived from the pairs (^{14}N)Py−^{20}Ne^{20}Ne/(^{14}N)Py−^{22}Ne^{20}Ne and (^{14}N)Py−^{20}Ne^{20}Ne/(^{14}N)Py−^{22}Ne^{22}Ne. Chutjian formulas for multiple substitution, used in the last case,[28] provide the same

TABLE 5: r_0 and r_s Structural van der Waals Parameters

	r_0	r_s
R^a (Å)	3.391(1)	3.355
θ^a (deg)	87.2(4)	85.8

[a] R and θ are referred to the center of mass of pyridine (see Figure 1).

results, within estimated errors, as the single substitution approach. The large-amplitude motions of the Ne atoms cause the imaginary values of *a*-coordinate of the N atom. However, one can deduce, from the smaller value of the *b*-coordinate of the N atom in the principal system of inertia of (^{14}N)Py−Ne_2, that the Ne atoms are shifted toward the N atom. This configuration is in accord with the one deduced, from plenty of experimental data, for Py−Ne.[8]

The corresponding r_s values of the van der Waals structural parameters (R and θ, see Figure 1), obtained by assuming zero for the *a*-coordinate of the N atom, are given in Table 5 and there compared to the r_0 values. These last values have been obtained by fitting simultaneously all 18 rotational constants. The values of the rotational constants calculated with the r_0 parameters are very close to the experimental values, with maximum deviations of 0.4% for the A rotational constants.

Only two independent parameters R and θ are required with the structure of the pyridine ring fixed to the geometrical parameters of the isolated molecule.

Conclusions

The rotational spectra of the six isotopologues of Py−Ne_2 are consistent with the [1,1] conformation of the complex, where the two Ne atoms are placed above and below the ring plane. The determined structural parameters R and θ are similar to those of Py−Ne ($R_0 = 3.400$ Å, $\theta_0 = 83.8°$), with the rare gas atoms shifted—with respect to the *c*-axis of isolated Py—toward the nitrogen atom of pyridine. The variations of R between the two different complexes are very small, while θ varies within 3°. Despite this difference in the bond angle, the possible presence of three-body nonadditive interactions could not be confirmed. Similarly, also in the complex Py−Ar_2 such three-body effects are not evident.

An unexpected slight increase of the rotational constant B ($\approx$0.25 MHz) in going from (^{14}N)Py−Ne_2 to (^{15}N)Py−Ne_2 is likely due to the zero-point energy level position being modified by large-amplitude van der Waals motions, but it is difficult to interpret quantitatively.

The quadrupole coupling constants (χ_{aa}, χ_{bb}, χ_{cc}) of (^{14}N)Py−Ne_2 (3.411, −4.853, and 1.442 MHz) are very similar to those of isolated pyridine[29] (−4.908, 1.434, and 3.474 MHz), when the above-mentioned inversion of axes is taken into account. The same set of constants for (^{14}N)Py−Ne (3.257, −4.706, and 1.450 MHz) presents larger deviations, mainly due to the fact that the *b*- (or *a*-) axis does not lie in the ring plane.

No lines attributable to the [2,0] isomer with both neon atoms on the same side of the ring plane have been identified. This could be due to conformational relaxation upon supersonic expansion[30] or to spectral complexity originated, for example, by an almost free rotation of the Ne_2 dimer with respect to Py.

Acknowledgment. We thank the University of Bologna for financial support.

Supporting Information Available: Tables of transition frequencies. This material is available free of charge via the Internet at http://pubs.acs.org.

References and Notes

(1) Caminati, W.; Grabow, J.-U. Microwave Spectroscopy: Molecular Systems. In *Frontiers of Molecular Spectroscopy*; Laane, J., Ed.; Elsevier: New York, 2008; Chapt. 15, p 508.
(2) Arunan, E.; Emilsson, T.; Gutowsky, H. S. *J. Chem. Phys.* **1994**, *101*, 861.
(3) Brupbacher, Th.; Makarewicz, J.; Bauder, A. *J. Chem. Phys.* **1994**, *101*, 9736.
(4) Brupbacher, Th.; Bauder, A. *Chem. Phys. Lett.* **1990**, *173*, 435.
(5) Klots, T. D.; Emilsson, T.; Gutowsky, H. S. *J. Chem. Phys.* **1992**, *97*, 5335.
(6) Tajaroon, C.; Jäger, W. *J. Chem. Phys.* **2007**, *12*, 034302.
(7) Maris, A.; Caminati, W.; Favero, P. G. *Chem. Commun. (Cambridge, U.K.)* **1998**, *23*, 2625.
(8) Velino, B.; Caminati, W. *J. Mol. Spectrosc.* **2008**, *251*, 176.
(9) Klots, T. D.; Emilsson, T.; Ruoff, R. S.; Gutowsky, H. S. *J. Phys. Chem.* **1989**, *93*, 1255.
(10) Spycher, R. M.; Petitprez, D.; Bettens, F. L.; Bauder, A. *J. Phys. Chem.* **1994**, *98*, 11863.
(11) Tang, S.; Evangelisti, L.; Velino, B.; Caminati, W. *J. Chem. Phys.* **2008**, *129*, 144301.
(12) Novick, S. E.; Harris, S. J.; Janda, K. C.; Klemperer, W. *Can. J. Phys.* **1975**, *53*, 2007.
(13) Caminati, W.; Millemaggi, A.; Favero, P. G.; Makarewicz, J. *J. Phys. Chem.* **1997**, *101*, 9272.
(14) Caminati, W.; Favero, P. G.; Melandri, S.; Meyer, R. *Chem.Phys. Lett.* **1997**, *268*, 393.
(15) Spycher, R. M.; King, P. M.; Bauder, A. *Chem. Phys. Lett.* **1991**, *177*, 371.
(16) Weber, Th.; Neusser, H. J. *J. Chem. Phys.* **1991**, *94*, 7689.
(17) Alberti, M.; Lagana', A.; Pirani, F.; Porrini, M.; Cappelletti, D *Lecture Notes Comput. Sci.* **2006**, *3980*, 721.
(18) Schmidt, M.; Mons, M.; Le Calvé, J. *Chem. Phys. Lett.* **1991**, *177*, 371.
(19) Schmidt, M.; Mons, M.; Le Calvé, J.; Millié, P.; Cossart-Magos, C. *Chem. Phys. Lett.* **1991**, *183*, 69.
(20) (a) Grabow, J.-U.; Stahl, W. *Z. Naturforsch. A* **1990**, *45*, 1043. (b) Grabow, J.-U. Doctoral thesis, Christian-Albrechts-Universität zu Kiel, Germany, 1992. (c) Grabow, J.-U.; Stahl, W.; Dreizler, H. *Rev. Sci. Instrum.* **1996**, *67*, 4072. (d) Grabow, J.-U. *Habilitationsschrift*; Universität Hannover, Hannover, Germany, 2004; http://www.pci.uni-hannover.de/~lgpca/spectroscopy/ftmw.
(21) Balle, T. J.; Flygare, W. H. *Rev. Sci. Instrum.* **1981**, *52*, 33.
(22) Caminati, W.; Millemaggi, A.; Alonso, J. L.; Lesarri, A.; López, J. C.; Mata, S. *Chem. Phys.Lett.* **2004**, *1*, 392.
(23) Pickett, H. M. *J. Mol. Spectrosc.* **1991**, *148*, 371.
(24) Watson, J. K. G. In *Vibrational Spectra and Structure*; Durig, J. R., Ed.; Elsevier: New York, 1977; Vol. 6, p 1.
(25) Xu, Y.; van Wijngaarden, J.; Jaeger, W. *Int. Rev. Phys. Chem.* **2005**, *24*, 301.
(26) Maris, A.; Favero, L. B.; Danieli, R.; Favero, P. G.; Caminati, W. *J. Chem. Phys.* **2000**, *113*, 8567.
(27) Kraitchmann, J. *Am. J. Phys* **1953**, *21*, 17.
(28) Chutjian, A. *J. Mol. Spectrosc.* **1964**, *14*, 361.
(29) Heineking, N.; Dreizler, H.; Schwarz, R. *Z. Naturforsch.* **1986**, *41a*, 1210.
(30) See, for example, Ruofft, R. S.; Klots, T. D.; Emilsson, T.; Gutowsky, H. S. *J. Chem. Phys.* **1990**, *93*, 3142.

JP902034K